

Hydrogen-bonded networks from η^5 -semiquinone complexes of manganese tricarbonyl

Moonhyun Oh, Jeffrey A. Reingold, Gene B. Carpenter, Dwight A. Sweigart*

Department of Chemistry, Brown University, Box H, Providence, RI 02912, USA

Received 27 June 2003; accepted 7 August 2003

Abstract

The cationic manganese tricarbonyl complexes containing η^6 -2-methylhydroquinone (**2a**), η^6 -2,3-dimethylhydroquinone (**3a**), η^6 -2-*t*-butylhydroquinone (**4a**), η^6 -tetramethylhydroquinone (**5a**) and η^6 -4,4'-biphenol (**6a**) are readily deprotonated to the corresponding neutral (η^5 -semiquinone) $\text{Mn}(\text{CO})_3$ (**2b–6b**) and anionic (η^4 -quinone) $\text{Mn}(\text{CO})_3^-$ (**2c–5c**) complexes. The X-ray structures of **2b–6b** feature strong intermolecular hydrogen bonding interactions that result in the formation of supramolecular organometallic networks. Significantly, the substitution pattern at the semiquinone ring affects the stereochemistry of the hydrogen bonding interactions. NMR spectra of **2b**, **3b** and **5b** reveal dynamic hydrogen bonding in solution.

© 2003 Elsevier B.V. All rights reserved.

Keywords: Hydrogen-bonded networks; Organometallic networks; η^5 -Semiquinone complexes; Manganese

1. Introduction

Substituted hydroquinones are fundamentally important in mediating electron and proton transfer reactions in biological systems [1]. The attachment of a metal unit to the π -system may well facilitate proton and electron transfer. There are, however, only few examples of complexes containing a hydroquinone ligand π -bonded to a transition metal [2,3]. This is due in part to a propensity [4] for quinone-type ligands to σ -bond to metals through the oxygen atoms rather than π -bond through the carbocyclic ring.

Previously, we reported that stable π -bonded hydroquinone, catechol and resorcinol complexes of manganese tricarbonyl could be obtained by reacting the free ligands with the manganese tricarbonyl transfer reagent [$(\eta^6$ -acenaphthene) $\text{Mn}(\text{CO})_3\text{BF}_4$] [3]. The $\text{Mn}(\text{CO})_3^+$ moiety in these complexes renders the $-\text{OH}$ protons quite acidic and the complexes are easily deprotonated with mild base to afford semiquinone and quinone complexes, as shown in Scheme 1. Interestingly, these

deprotonations can be viewed as being coupled with electron transfer from the quinonoid ring to the attached manganese moiety, which serves as an internal oxidant.

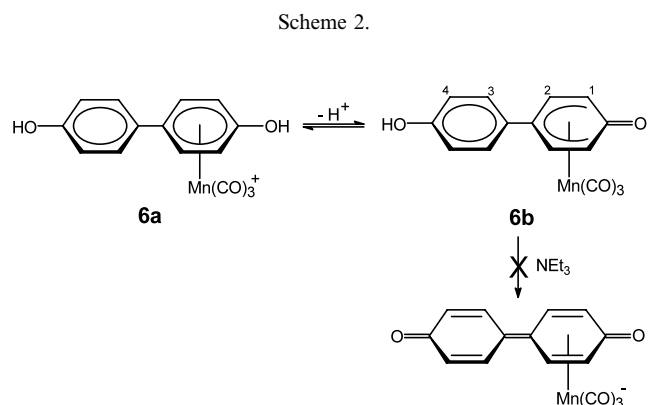
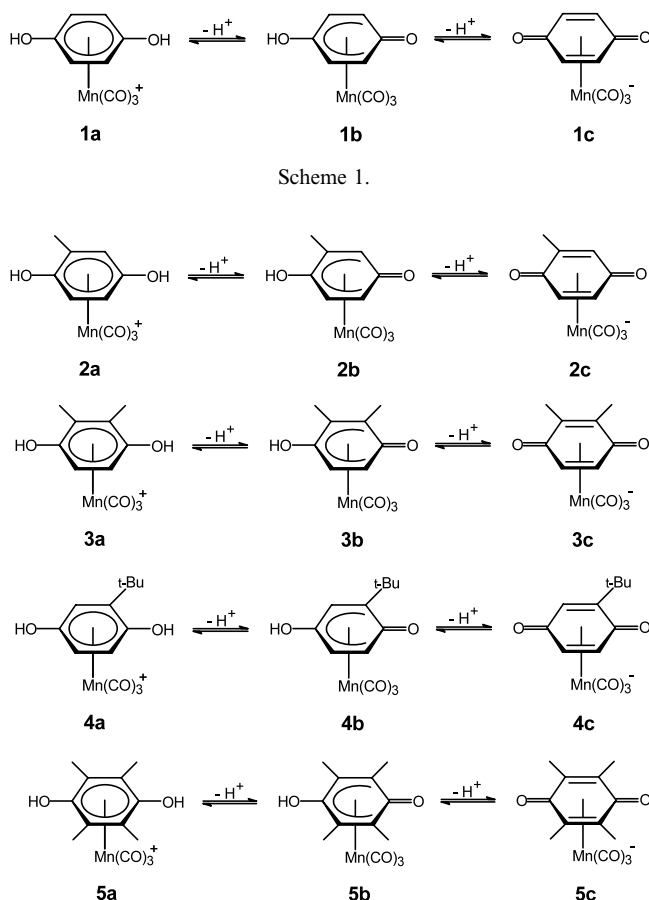
Herein we report the synthesis and deprotonation chemistry of π -coordinated complexes **2a–6a** containing the hydroquinone-type ligands indicated in Schemes 2 and 3. The crystal structures of **2b–6b** reveal that these complexes exist as organometallic polymers due to strong intermolecular hydrogen bonding interactions. Significantly, it is demonstrated that the substitution pattern on the semiquinone ring affects the stereochemistry with which the semiquinone C=O oxygen lone pair interacts with the $-\text{OH}$ group in the adjacent molecule.

2. Results and discussion

As with complex **1a**, complexes **2a–6a** were easily made as the BF_4^- salt by reaction of the appropriate hydroquinone ligand with the manganese tricarbonyl transfer reagent [$(\eta^6$ -acenaphthene) $\text{Mn}(\text{CO})_3\text{BF}_4$] [5]. Complexes **2a–6a** are very stable in solution and in the solid state and were fully characterized by IR and NMR spectroscopy. Complexes **2a–6a** undergo spontaneous proton dissociation in DMSO to give a mixture of

* Corresponding author. Tel.: +1-401-8632767; fax: +1-401-8632594.

E-mail address: dwight_sweigart@brown.edu (D.A. Sweigart).



2a–6a and the corresponding η^5 -semiquinone species **2b–6b**, as was previously demonstrated with the unsubstituted complex **1a**. This reversible proton loss is illustrated in Scheme 2. It was found that both single and double deprotonation of **2a–5a** could be conveniently and reversibly effected by the addition of the weak base NEt_3 . In contrast, the acidity of the OH group in **6b** is too weak to allow deprotonation by NEt_3 (Scheme 3). This is undoubtedly due to the inability of the $\text{Mn}(\text{CO})_3^+$ moiety to sufficiently activate an arene ring adjacent to the one coordinated to the metal.

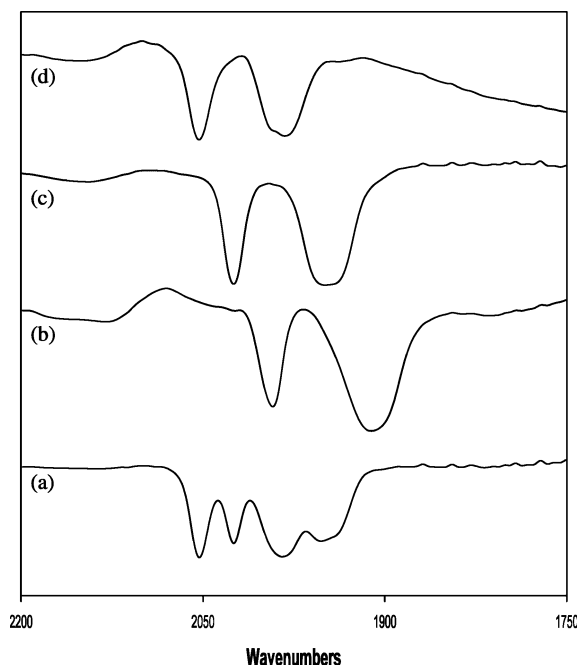
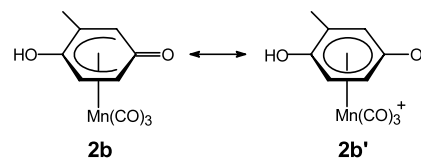


Fig. 1. IR spectra in DMSO showing reversible of deprotonation/protonation of complex **2a** according to Scheme 2. Spectrum (a), complex **2a** dissolved in DMSO showing dissociation into an equilibrium mixture of **2a** and **2b**; (b), addition of NEt_3 generates **2c**; (c), addition of $\text{HBF}_4 \cdot \text{Et}_2\text{O}$ to (b) protonates **2c** to form **2b**; (d), addition of more $\text{HBF}_4 \cdot \text{Et}_2\text{O}$ protonates **2b** to form **2a**.

A typical experiment is illustrated in Fig. 1 for complex **2a**. Spectrum (a) shows that **2a** is ca. 50% converted to **2b** in pure DMSO. Spectrum (b) reveals that several equivalents of NEt_3 changes **2a** to the quinone complex **2c**, which can be reprotonated to **2b** with an equivalent of $\text{HBF}_4 \cdot \text{Et}_2\text{O}$, as shown in spectrum (c). Additional $\text{HBF}_4 \cdot \text{Et}_2\text{O}$ transforms **2b** to **2a** as shown in spectrum (d). All five neutral η^5 -coordinated semiquinone complexes **2b–6b** were found to be stable in solution and in the solid state. The anionic quinone complexes **2c–5c** are stable in solution, although they could not be isolated as the HNEt_3^+ salts.

The neutral η^5 -semiquinone complex **2b** was obtained in good yield by adding an equivalent of NEt_3 to a solution of $[\mathbf{2a}]\text{BF}_4$ in acetone. The ν_{CO} bands of **2b** are ca. 18 wavenumbers higher than that normally found for (η^5 -cyclohexadienyl) $\text{Mn}(\text{CO})_3$ complexes [6], a fact that we ascribe to a significant contribution from the η^6 -resonance form **2b'** shown below.



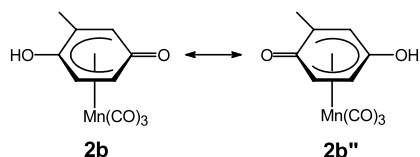
The NMR spectra of **2b**, **3b** and **5b** indicate dynamic, strong hydrogen bonding in solution. There is, however, no evidence of dynamic hydrogen bonding interactions

in solution for **4b** and **6b**. The $^1\text{H-NMR}$ spectrum of **2b** shows just one broad signal at 5.47 ppm for the three aromatic protons, which suggests dynamic hydrogen bonding that has the effect of ‘mixing’ the C–OH and the C=O ends of the molecule (Scheme 4). The signals for the methyl and hydroxy groups appear at 1.97 and 10.47 ppm, respectively.

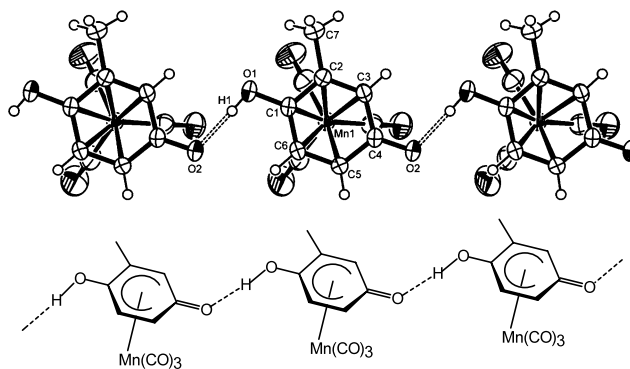
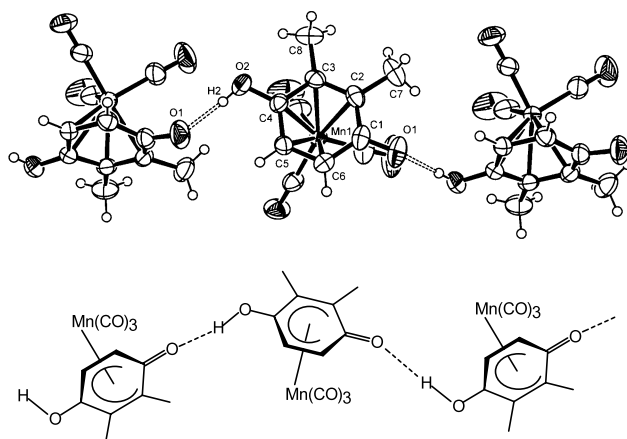
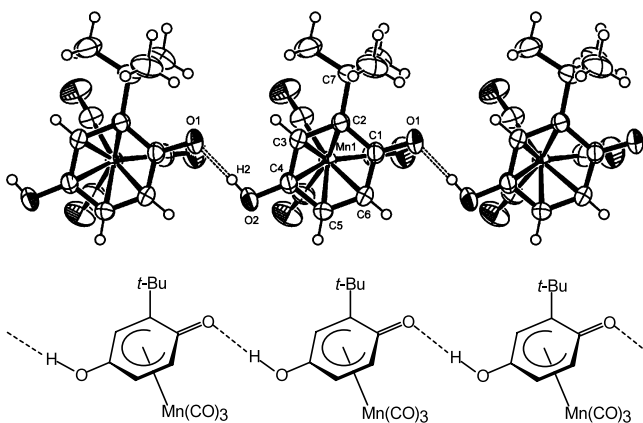
The $^1\text{H-NMR}$ spectrum of **3b** also gives evidence for dynamic hydrogen bonding interactions, with only one signal at 5.23 ppm for the two aromatic protons and one signal at 2.16 ppm for the two methyl groups present in the $^1\text{H-NMR}$. Complex **5b** has a singlet at 2.08 ppm for four equivalents methyl groups in proton NMR, which again indicates the presence of dynamic hydrogen bonding in solution.

The $^1\text{H-NMR}$ data of **4b**, however, suggests that there is no dynamic hydrogen bonding interaction in solution. A singlet for H1 and doublet for H2 are present at 6.17 and 6.13 ppm, respectively, while an upfield doublet for H3 is found at 4.54 ppm. While there is no evidence for dynamic hydrogen interaction in solution, the X-ray structure revealed that there are linear chains of strongly hydrogen-bonded semiquinone molecules in the solid state, just as with **2b** and **3b** (vide infra). This lack of dynamic hydrogen bonding in solution for **4b** is possibly due to steric effects attributable to the *t*-butyl substituent.

Crystal structures were determined for all five η^5 -semiquinone complexes **2b**–**6b**. The structures are shown in Figs. 2–6 and crystal data, along with selected bond lengths and angles, are given in Tables 1–4. With all five complexes, the most interesting feature is the presence of intermolecular hydrogen bonding that leads to 1D supramolecular chain structures. As shown in Table 5, the hydrogen-bonded O–O donor–acceptor distances are remarkably short and can be compared to the O–O distance of 2.74 Å reported for the hydrogen-bonded dimer consisting of hydroquinone and quinone [7]. The hydrogen bonding has the effect of ‘mixing’ the C–OH and the C=O ends of the molecule with the consequence that both bend or ‘envelope’ out of the plane defined by C(2)–C(3)–C(5)–C(6) in complexes **2b**–**5b**. Thus, both planes defined by C(3)–C(4)–C(5) and C(2)–C(1)–C(6) are bent up by ca. 5–10°. The interplanar angles between these planes and the C(2)–C(3)–C(5)–C(6) plane is much less than that seen in typical (cyclohexadienyl) $\text{Mn}(\text{CO})_3$ complexes [6] as well as that found in (η^5 -pentamethylbenzyl) $\text{Mn}(\text{CO})_3$ [8]



Scheme 4.

Fig. 2. Crystal structure of **2b** with thermal ellipsoids at the 50% probability level.Fig. 3. Crystal structure of **3b** with thermal ellipsoids at the 50% probability level.Fig. 4. Crystal structure of **4b** with thermal ellipsoids at the 50% probability level.

and (η^5 -oxocyclohexadienyl) $\text{Mn}(\text{CO})_3$ [9]. In concert with this, the Mn–C(1) [or Mn–C(4)] distances are short enough to indicate some bonding interaction at the C=O link, although less than that which occurs at the C–OH end of the ring (see Tables 1–4). Complex **6b** differs from the others in that the C–OH and the C=O

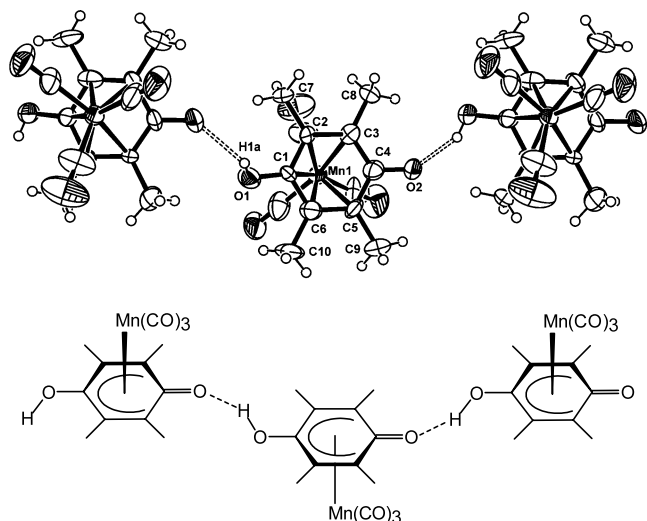


Fig. 5. Crystal structure of **5b** with thermal ellipsoids at the 50% probability level.

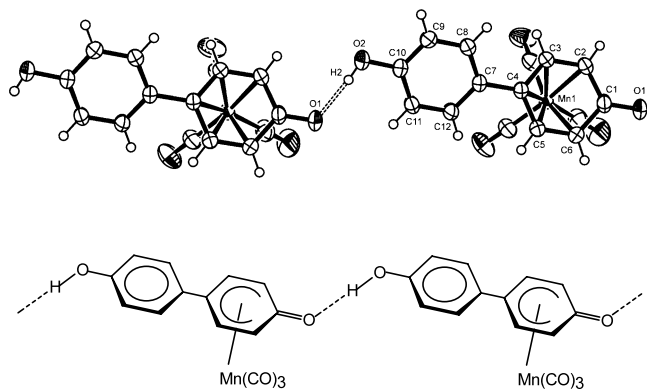
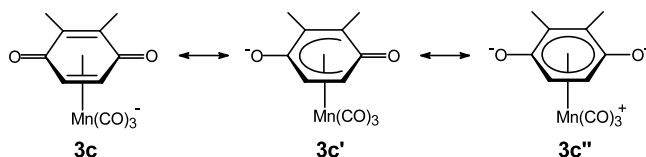


Fig. 6. Crystal structure of **6b** with thermal ellipsoids at the 50% probability level.

ends of the molecule are not ‘similar’ as in the other semiquinone complexes. The consequence of this that the Mn–C(1) distance in **6b** (2.45 Å) is longer than the corresponding distances in **2b–5b** (average 2.38 Å), indicative of the expected diminished interaction.

Another interesting structural feature of **2b–6b** is the stereochemistry of the polymer networks. The hydrogen bonding is extended in a *cis*-fashion in **3b** and **5b**, as shown in Figs. 3 and 5. With **2b**, **4b**, and **6b**, however, the hydrogen bonding pattern is *trans* (Figs. 2, 4 and 6). Thus, the oxygen lone pairs function in a stereochemically active manner that seems to be largely dictated by the steric influences of the ring substituents.

Deprotonation of the semiquinone complexes **2b–5b** was found to be facile in DMSO using NEt_3 as the base (see Fig. 1). Isolation of the product quinone salts **2c–5c** proved to be difficult with HNEt_3^+ as the counterion, but deprotonation with alkali metal acetates led to stable metal salts. As in the case of the semiquinones, IR spectra of **2c–5c** show ν_{CO} bands at wavenumbers



Scheme 5.

considerably higher than those reported for other anionic $(\eta^4\text{-diene})\text{Mn}(\text{CO})_3^-$ complexes, e.g. $(\eta^4\text{-naphthalene})\text{Mn}(\text{CO})_3^-$ and $(\eta^4\text{-xylylene})\text{Mn}(\text{CO})_3^-$ [10]. In the case of **3c**, for example, we interpret this to mean that resonance forms **3c'** and **3c''** shown in Scheme 5 make a nontrivial contribution.

We previously demonstrated that **1c** (QMTC) interacts with a wide variety of metal ions by σ -bonding through the oxygen atoms to afford metal–organometallic coordination networks (MOMNs) [11]. One can anticipate that anionic complexes **2c–5c** could also act as spacers to generate MOMNs. The substituent-induced hydrogen bonding patterns observed in the present work may be useful for predicting the architecture of metal–organometallic networks based on π -bonded quinone spacers. Indeed, it has recently been shown that the stereochemical switch from *trans* to *cis* observed in the hydrogen bonding pattern upon going from **1b** to **3b** is closely mimicked when the **1c** and **3c** analogues are used as spacers to bind to divalent metal ions [12].

3. Experimental

3.1. General

Standard materials were purchased from commercial sources and used without further purification. Acetone and dichloromethane solvents were HPLC grade and opened under nitrogen. ^1H - and ^{13}C -NMR spectra were recorded on Bruker 300 and 400 MHz instruments. 2,3,5,6-Tetramethylhydroquinone is synthesized from duroquinone using the Allen synthesis [13].

3.2. Synthesis of the cationic η^6 -coordinated complexes of manganese tricarbonyl **2a–6a**

$[(\eta^6\text{-2-Me-hydroquinone})\text{Mn}(\text{CO})_3]\text{BF}_4$ (**2a**) BF_4 was synthesized by treating the manganese tricarbonyl transfer reagent $[(\eta^6\text{-acenaphthene})\text{Mn}(\text{CO})_3]\text{BF}_4$ with 2-methylhydroquinone according to a published procedure [3]. 2-Methylhydroquinone (0.3 g) was added to a solution of $[(\eta^6\text{-acenaphthene})\text{Mn}(\text{CO})_3]\text{BF}_4$ (0.5 g) in CH_2Cl_2 (ca. 15 ml) under N_2 . The mixture was sealed in a pressure bottle and heated to 70 °C for 2 h. The reaction mixture was then cooled to room temperature (r.t.). Finally, the precipitated pale yellow powder was

Table 1
Crystallographic data for semiquinone complexes **2b–6b**

	2b	3b	4b	5b	6b
Empirical Formula	C ₁₀ H ₇ MnO ₅	C ₁₁ H ₉ MnO ₅	C ₁₃ H ₁₃ MnO ₅	C ₁₃ H ₁₃ MnO ₅	C ₁₅ H ₉ MnO ₅
Formula weight	262.10	276.12	304.17	304.17	324.16
Temperature (K)	298	298	298	298	298
Wavelength (Å)	0.71073	0.71073	0.71073	0.71073	0.71073
Crystal system	Triclinic	Monoclinic	Monoclinic	Triclinic	Triclinic
Space group	<i>P</i> $\bar{1}$	<i>P</i> 2 ₁ / <i>c</i>	<i>P</i> 2 ₁ / <i>n</i>	<i>P</i> $\bar{1}$	<i>P</i> $\bar{1}$
<i>a</i> (Å)	6.8520(5)	8.9201(5)	6.8500(3)	14.2320(12)	6.7260(7)
<i>b</i> (Å)	7.6545(5)	9.1943(6)	12.8279(6)	18.7943(17)	9.7440(10)
<i>c</i> (Å)	10.2065(7)	13.8435(8)	15.3869(7)	20.2411(18)	10.2105(10)
α (°)	92.0890(10)	90	90	81.564(2)	94.198(2)
β (°)	92.6330(10)	95.8350(10)	101.7330(10)	87.568(2)	100.262(2)
γ (°)	106.8000(10)	90	90	86.787(2)	96.140(2)
<i>V</i> (Å ³)	511.24(6)	1129.48(12)	1323.8(10)	5343.9(8)	651.78(11)
<i>Z</i>	2	4	4	16	2
<i>D</i> _{calc} (g cm ⁻³)	1.703	1.624	1.526	1.512	1.652
μ (mm ⁻¹)	1.292	1.174	1.009	1.000	1.031
<i>F</i> (000)	264	560	624	2496	328
Crystal dimension (mm)	0.23 × 0.22 × 0.20	0.38 × 0.32 × 0.28	0.50 × 0.20 × 0.19	0.34 × 0.17 × 0.07	0.28 × 0.24 × 0.11
θ Range (°)	2.00–28.28	2.30–28.28	2.70–28.30	2.04–26.51	2.11–28.30
Reflections collected	5509	11 447	13 994	66 771 ^a	6963
Independent reflections	2487 (<i>R</i> _{int} = 0.0169)	2787 (<i>R</i> _{int} = 0.0187)	3264 (<i>R</i> _{int} = 0.0196)	66 771 (<i>R</i> _{int} = 0.000) ^a	3136 (<i>R</i> _{int} = 0.0250)
Data/restraints/parameters	2487/0/146	2787/0/156	3264/0/175	66 771/0/1402	3136/0/190
<i>R</i> ₁ , <i>wR</i> ₂ [<i>I</i> > 2 σ (<i>I</i>)]	0.0362, 0.0945	0.0310, 0.0833	0.0310, 0.0822	0.0594, 0.1179	0.0370, 0.1027
<i>R</i> ₁ , <i>wR</i> ₂ (all data)	0.0391, 0.0964	0.0362, 0.0876	0.0348, 0.0850	0.1596, 0.1395	0.0411, 0.1055
Goodness-of-fit on <i>F</i> ²	1.091	1.030	1.068	0.782	1.086

^a The seemingly large number of reflections is a consequence of software used to account for crystal twinning.

Table 2
Selected bond distances (Å) and angles (°) for complexes **2b** and **3b**

2b	3b		
<i>Bond distances</i>			
Mn(1)–C(1)	2.2341(18)	Mn(1)–C(1)	2.2310(15)
Mn(1)–C(2)	2.2065(18)	Mn(1)–C(2)	2.2086(15)
Mn(1)–C(3)	2.1962(17)	Mn(1)–C(3)	2.2235(15)
Mn(1)–C(4)	2.3673(18)	Mn(1)–C(4)	2.3777(16)
Mn(1)–C(5)	2.193(2)	Mn(1)–C(5)	2.1880(17)
Mn(1)–C(6)	2.165(2)	Mn(1)–C(6)	2.1651(15)
C(1)–O(1)	1.327(2)	C(1)–O(1)	1.3360(18)
C(4)–O(2)	1.269(2)	C(4)–O(2)	1.267(2)
<i>Bond angles</i>			
O(1)–C(1)–C(6)	123.25(16)	O(1)–C(1)–C(6)	123.09(14)
O(1)–C(1)–C(2)	118.74(16)	O(1)–C(1)–C(2)	117.68(15)
O(2)–C(4)–C(5)	122.66(17)	O(2)–C(4)–C(5)	121.89(18)
O(2)–C(4)–C(3)	122.57(15)	O(2)–C(4)–C(3)	122.45(17)
C(6)–C(1)–C(2)	117.95(15)	C(6)–C(1)–C(2)	119.20(13)
C(3)–C(2)–C(1)	119.45(16)	C(3)–C(2)–C(1)	119.12(15)
C(2)–C(3)–C(4)	123.38(15)	C(2)–C(3)–C(4)	121.61(14)
C(5)–C(4)–C(3)	114.47(15)	C(5)–C(4)–C(3)	115.44(14)
C(6)–C(5)–C(4)	121.10(17)	C(6)–C(5)–C(4)	121.84(15)
C(5)–C(6)–C(1)	121.89(16)	C(1)–C(6)–C(5)	120.76(15)

Table 3
Selected bond distances (Å) and angles (°) for complexes **4b** and **5b**

4b	5b		
<i>Bond distances</i>			
Mn(1)–C(1)	2.3909(13)	Mn(1)–C(1)	2.203(4)
Mn(1)–C(2)	2.2366(13)	Mn(1)–C(2)	2.198(4)
Mn(1)–C(3)	2.1649(13)	Mn(1)–C(3)	2.196(4)
Mn(1)–C(4)	2.2324(13)	Mn(1)–C(4)	2.401(5)
Mn(1)–C(5)	2.1728(14)	Mn(1)–C(5)	2.216(4)
Mn(1)–C(6)	2.1897(14)	Mn(1)–C(6)	2.192(4)
C(1)–O(1)	1.2702(16)	C(1)–O(1)	1.364(4)
C(4)–O(2)	1.3259(15)	C(4)–O(2)	1.243(4)
<i>Bond angles</i>			
O(1)–C(1)–C(6)	121.04(13)	O(1)–C(1)–C(6)	115.5(4)
O(1)–C(1)–C(2)	122.91(13)	O(1)–C(1)–C(2)	122.9(4)
O(2)–C(4)–C(3)	124.13(13)	O(2)–C(4)–C(3)	122.2(4)
O(2)–C(4)–C(5)	118.64(13)	O(2)–C(4)–C(5)	123.1(4)
C(6)–C(1)–C(2)	115.73(11)	C(6)–C(1)–C(2)	121.5(4)
C(3)–C(2)–C(1)	118.06(12)	C(3)–C(2)–C(1)	117.8(4)
C(4)–C(3)–C(2)	123.69(12)	C(4)–C(3)–C(2)	123.0(4)
C(3)–C(4)–C(5)	117.16(11)	C(3)–C(4)–C(5)	114.4(4)
C(6)–C(5)–C(4)	120.14(12)	C(6)–C(5)–C(4)	121.2(4)
C(5)–C(6)–C(1)	122.98(12)	C(5)–C(6)–C(1)	119.7(4)

collected by filtration, washed with CH₂Cl₂ and dried in vacuo. For [**2a**]BF₄: yield 87%. IR (Me₂SO): ν_{CO} 2055 (s), 1988 (s, br) cm⁻¹. IR (acetone): ν_{CO} 2064 (s), 2001 (s, br) cm⁻¹. ¹H-NMR (CD₃CN): δ 6.19 (d, *J* = 7.43 Hz, *H*₃, 1H), 6.05 (d, *J* = 2.25 Hz, *H*₁, 1H), 5.81 (dd, *J* =

7.43, 2.25 Hz, *H*₂, 1H), 2.32 (s, *CH*₃, 3H). ¹H-NMR (*d*₆-acetone): δ 6.57 (d, *J* = 7.46 Hz, *H*₃, 1H), 6.48 (d, *J* = 2.81 Hz, *H*₁, 1H), 6.18 (dd, *J* = 7.46, 2.81 Hz, *H*₂, 1H), 2.32 (s, *CH*₃, 3H). ¹³C-NMR (CD₃CN): δ 218.2 (Mn–CO), 139.8, 135.1, 107.6, 89.0, 87.3, 82.9, 15.8 (*CH*₃).

Table 4
Selected bond distances (Å) and angles (°) for complex **6b**

Bond distances			
Mn(1)–C(1)	2.4468(18)	Mn(1)–C(5)	2.1587(16)
Mn(1)–C(2)	2.2132(17)	Mn(1)–C(6)	2.2115(18)
Mn(1)–C(3)	2.1502(17)	C(1)–O(1)	1.251(2)
Mn(1)–C(4)	2.1936(17)	C(10)–O(2)	1.348(2)
Bond angles			
O(1)–C(1)–C(2)	124.24(17)	C(3)–C(2)–C(1)	122.23(15)
O(1)–C(1)–C(6)	122.47(17)	C(2)–C(3)–C(4)	122.17(15)
O(2)–C(10)–C(9)	118.65(16)	C(3)–C(4)–C(5)	115.66(15)
O(2)–C(10)–C(11)	121.97(17)	C(6)–C(5)–C(4)	122.35(16)
C(2)–C(1)–C(6)	112.87(15)	C(5)–C(6)–C(1)	122.11(16)

Table 5
Hydrogen bond parameters for the semiquinone complexes **1b–6b**

Complexes	D–H···A	<i>d</i> (D···A)	<(DHA)
1b [3]	O(1)–	2.47	172.8
	H(1)···O(2)		
(η ⁵ - <i>o</i> -Semiquinone)Mn(CO) ₃ [3]	O(2)–	2.63	153.7
	H(2)···O(1)		
2b	O(1)–	2.52	176.1
	H(1)···O(2)		
3b	O(1)–	2.54	173.6
	H(1)···O(2)		
4b	O(2)–	2.48	174.7
	H(2)···O(1)		
5b	O(1)–	2.53	141.3
	H(1)···O(7)		
6b	O(2)–	2.63	171.8
	H(2)···O(1)		

To synthesize complexes **3a–6a**, the same procedure used for the synthesis of **2a** was followed. For [**3a**]BF₄: yield 88%. IR (Me₂SO): ν_{CO} 2053 (s), 1985 (s, br) cm⁻¹. IR (acetone): ν_{CO} 2061 (s), 1997 (s, br) cm⁻¹. ¹H-NMR (*d*₆-acetone): δ 7.37 (OH), 6.31 (s, *H*₁, 2H), 2.53 (s, *CH*₃, 6H). ¹H-NMR (*d*₆-Me₂SO): δ 5.85 (s, *H*₁, 2H), 2.23 (s, *CH*₃, 6H). For [**4a**]BF₄: yield 90%. IR (Me₂SO): ν_{CO} 2054 (s), 1987 (s, br) cm⁻¹. IR (acetone): ν_{CO} 2062 (s), 1999 (s, br) cm⁻¹. IR (CH₃CN): ν_{CO} 2065 (s), 2003 (s, br) cm⁻¹. ¹H-NMR (CD₃CN): δ 8.69 (br, OH, 1H), 6.34 (d, *J* = 2.11 Hz, *H*₁, 1H), 6.27 (dd, *J* = 7.58, 2.11 Hz, *H*₂, 1H), 5.90 (d, *J* = 7.58 Hz, *H*₃, 1H), 1.43 (s, C(*CH*₃)₃, 9H). ¹H-NMR (CD₃OD): δ 6.28 (d, *J* = 2.18 Hz, *H*₁, 1H), 6.24 (dd, *J* = 7.63, 2.18 Hz, *H*₂, 1H), 5.59 (d, *J* = 7.63 Hz, *H*₃, 1H), 1.39 (s, C(*CH*₃)₃, 9H). ¹³C-NMR (CD₃CN): δ 218.3 (Mn–CO), 140.2, 134.3, 114.4, 89.7, 89.5, 85.2, 35.9 (C(*CH*₃)₃), 29.6 (C(*CH*₃)₃). ¹³C-NMR (CD₃OD): δ 219.3 (Mn–CO), 142.8, 135.3, 114.0, 90.7, 89.5, 84.8, 36.0 (C(*CH*₃)₃), 29.8 (C(*CH*₃)₃). For [**5a**]BF₄: yield 94%. IR (CH₃CN): ν_{CO} 2059 (s), 1995 (s, br) cm⁻¹. ¹H-NMR (CD₃CN): δ 2.07 (s, *CH*₃, 12H). For [**6a**]BF₄: yield 82%. IR (CH₃CN): ν_{CO} 2071 (s), 1912 (s, br) cm⁻¹. IR (acetone): ν_{CO} 2068 (s), 2010 (s, br)

cm⁻¹. ¹H-NMR (*d*₆-acetone): δ 7.74 (d, *J* = 8.48 Hz, *H*₃, 2H), 7.30 (d, *J* = 7.30 Hz, *H*₂, 2H), 7.00 (d, *J* = 8.48 Hz, *H*₄, 2H), 6.10 (d, *J* = 7.30 Hz, *H*₁, 2H).

3.3. Synthesis of the neutral η⁵-coordinated complexes of manganese tricarbonyl **2b–6b**

Triethylamine (0.33 mmol) was added to a solution of [**2a**]BF₄ (100 mg, 0.29 mmol) in acetone (10 ml) under nitrogen at r.t. After removing some acetone solvent by bubbling N₂, a pale yellow precipitate of **2b** formed, which was filtered and washed three times with acetone and dried in vacuo. Yield 75%. IR (Me₂SO): ν_{CO} 2028 (s), 1950 (s, br) cm⁻¹. ¹H-NMR (*d*₆-Me₂SO): δ 10.47 (br, OH, 1H), 5.47 (br, aromatic protons, 3H), 1.97 (s, 3H). To synthesize complexes **3b–6b**, the same procedure used for the synthesis of **2b** was followed, except **5b**. For **5b**, the acetone solvent was removed and the product taken up in dichloromethane and precipitated with diethyl ether. For **3b**: yield 78%. IR (Me₂SO): ν_{CO} 2025 (s), 1948 (s, br) cm⁻¹. IR (acetone): ν_{CO} 2028 (s), 1947 (s, br) cm⁻¹. IR (CH₂Cl₂): ν_{CO} 2038 (s), 1965 (s, br) cm⁻¹. ¹H-NMR (*d*₆-Acetone): δ 5.23 (br, *H*₁ and *H*₂, 2H), 2.16 (s, 2(*CH*₃), 6H). For **4b**: yield 88%. IR (Me₂SO): ν_{CO} 2025 (s), 1941 (s, br) cm⁻¹. ¹H-NMR (*d*₆-Me₂SO): δ 10.33 (br, OH, 1H), 6.17 (s, *H*₁, 1H), 6.13 (d, *J* = 7.63 Hz, *H*₂, 1H), 4.54 (d, *J* = 7.63 Hz, *H*₃, 1H), 1.26 (s, C(*CH*₃)₃, 9H). ¹³C-NMR (*d*₆-Me₂SO): δ 221.9 (Mn–CO), 163.5, 125.5, 107.5, 91.8, 78.3, 34.3 (C(*CH*₃)₃), 28.9 (C(*CH*₃)₃). For **5b**: yield 45%. IR (CH₃CN): ν_{CO} 2026 (s), 1953 (s, br) cm⁻¹. ¹H-NMR (CD₃CN): δ 2.08 (s, *CH*₃, 12H). For **6b**: yield 82%. IR (Me₂SO): ν_{CO} 2036 (s), 1965 (s, br) cm⁻¹. ¹H-NMR (*d*₆-Me₂SO): δ 9.83 (br, OH, 1H), 7.57 (d, *J* = 8.23 Hz, *H*₃, 2H), 6.86 (d, *J* = 7.83 Hz, *H*₂, 2H), 6.83 (d, *J* = 8.23 Hz, *H*₄, 2H), 4.89 (d, *J* = 7.83 Hz, *H*₁, 2H). ¹H-NMR (*d*₆-acetone): δ 7.63 (d, *J* = 8.46 Hz, *H*₃, 2H), 6.93 (d, *J* = 8.46 Hz, *H*₄, 2H), 6.79 (d, *J* = 7.79 Hz, *H*₂, 2H), 4.92 (d, *J* = 7.79 Hz, *H*₁, 2H). ¹³C-NMR (*d*₆-Me₂SO): δ 220.1 (Mn–CO), 166.0, 158.3, 127.7, 124.2, 115.8, 103.4, 95.9, 82.9.

3.4. Synthesis of the anionic η⁴-coordinated complexes **2c–5c**

The HNEt₃⁺ salts of the anionic quinone complexes **2c–5c**, were synthesized by the addition of excess NEt₃ (at least two equivalents) to η⁶-complexes **2a–5a** or by the addition of NEt₃ to η⁵-complexes **2b–5b**. The products could not be isolated as solids because they easily convert to semiquinone complexes. For [**2c**]HNEt₃, IR (Me₂SO): ν_{CO} 1996 (s), 1915 (s, br) cm⁻¹. ¹H-NMR (*d*₆-Me₂SO): δ 5.09 (br, 1H), 4.94 (br, 1H), 4.76 (br, 1H), 1.86 (s, *CH*₃, 3H), 2.69 (N(*CH*₂*CH*₃)₃, 6H), 1.02 (N(*CH*₂*CH*₃)₃, 9H). For [**3c**]HNEt₃, IR (Me₂SO): ν_{CO} 1993 (s), 1911 (s, br) cm⁻¹. For [**4c**]HNEt₃, IR (Me₂SO): ν_{CO} 1993 (s), 1915

(s, br) cm^{-1} . $^1\text{H-NMR}$ ($d_6\text{-Me}_2\text{SO}$): δ 5.24 (br, 1H), 5.33 (br, 1H), 4.40 (br, 1H) 1.24 (s, $\text{C}(\text{CH}_3)_3$, 9H), 2.74 ($\text{N}(\text{CH}_2\text{CH}_3)_3$, 6H), 1.04 ($\text{N}(\text{CH}_2\text{CH}_3)_3$, 9H). For [5c]HNEt₃, IR (Me_2SO): ν_{CO} 1983 (s), 1900 (s, br) cm^{-1} .

3.5. Crystal structures

X-ray data collection with Mo-K_α radiation was carried out at 298 K using a Bruker Apex diffractometer equipped with a CCD area detector. Structures were determined by direct methods and refined on F^2 . All hydrogen atoms were inserted in ideal positions, riding on their carbon atoms.

4. Supplementary material

X-ray crystallographic data have been deposited with the Cambridge Crystallographic Data Centre, CCDC nos. 213260–213264 for complexes **2b**–**6b**. Copies of this information may be obtained free of charge from The Director, CCDC, 12 Union Road, Cambridge CB2 1EZ, UK (Fax: +44-1223-336033; e-mail: deposit@ccdc.cam.ac.uk or www: <http://www.ccdc.cam.ac.uk>).

Acknowledgements

Acknowledgment is made to the donors of The American Chemical Society Petroleum Research Fund for support of this research.

References

- [1] G. Lenaz (Ed.), Coenzyme Q: Biochemistry, Bioenergetics and Clinical Applications of Ubiquinone, John Wiley & Sons, New York, 1985.
- [2] (a) M.E. Wright, *J. Organomet. Chem.* 376 (1989) 353; (b) H. Schumann, A.M. Arif, T.G. Richmond, *Polyhedron* 9 (1990) 1677;
- (c) G. Fairhurst, C. White, *J. Chem. Soc. Dalton Trans.* (1979) 1531;
- (d) Y.-S. Huang, S. Sabo-Etienne, X.-D. He, B. Chaudret, *Organometallics* 11 (1992) 3031;
- (e) U. Koelle, C. Weisschädel, U. Englert, *J. Organomet. Chem.* 490 (1995) 101;
- (f) S. Sun, G.B. Carpenter, D.A. Sweigart, *J. Organomet. Chem.* 512 (1996) 257;
- (g) J. Le Bras, H. Amouri, J. Vaissermann, *Organometallics* 17 (1998) 1116.
- [3] M. Oh, G.B. Carpenter, D.A. Sweigart, *Organometallics* 21 (2002) 1290.
- [4] (a) C.G. Pierpont, C.W. Langi, *Prog. Inorg. Chem.* 41 (1994) 331; (b) O.-S. Jung, D.H. Jo, Y.A. Lee, B.J. Conklin, C.G. Pierpont, *Inorg. Chem.* 36 (1997) 19; (c) D.M. Adams, D.N. Hendrickson, *J. Am. Chem. Soc.* 118 (1996) 11515; (d) F. Hartl, A. Vlcek, *Inorg. Chem.* 35 (1996) 1257.
- [5] S. Sun, L.K. Yeung, D.A. Sweigart, T.-Y. Lee, S.S. Lee, Y.K. Chung, S.R. Switzer, R.D. Pike, *Organometallics* 14 (1995) 2613.
- [6] (a) M.R. Churchill, S. Scholer, *Inorg. Chem.* 8 (1969) 1950; (b) S.D. Ittel, J.F. Whitney, Y.K. Chung, P.G. Williard, D.A. Sweigart, *Organometallics* 7 (1988) 1323; (c) T.-Y. Lee, H.-K. Bae, Y.K. Chung, W.A. Hallows, D.A. Sweigart, *Inorg. Chim. Acta* 224 (1994) 147.
- [7] T. Sakurai, *Acta Crystallogr. B* 24 (1968) 403.
- [8] D.M. LaBrush, D.P. Eyman, N.C. Baenziger, L.M. Mallis, *Organometallics* 10 (1991) 1026.
- [9] S.-G. Lee, J.-A. Kim, Y.K. Chung, T.-S. Yoon, N. Kim, W. Shin, *Organometallics* 14 (1995) 1023.
- [10] (a) R.L. Thompson, S. Lee, A.L. Rheingold, N.J. Cooper, *Organometallics* 10 (1991) 1657; (b) J.W. Hull, K.J. Roesselet, W.L. Gladfelter, *Organometallics* 11 (1992) 3630.
- [11] (a) M. Oh, G.B. Carpenter, D.A. Sweigart, *Angew. Chem. Int. Ed.* 40 (2001) 3191; (b) M. Oh, G.B. Carpenter, D.A. Sweigart, *Angew. Chem. Int. Ed.* 41 (2002) 3650; (c) M. Oh, G.B. Carpenter, D.A. Sweigart, *Angew. Chem. Int. Ed.* 42 (2003) 2026; (d) M. Oh, G.B. Carpenter, D.A. Sweigart, *Chem. Commun.* (2002) 2168.
- [12] M. Oh, G.B. Carpenter, D.A. Sweigart, *Organometallics* 22 (2003) 2364.
- [13] J.F. Allen, P. Horton, *Biochim. Biophys. Acta* 638 (2) (1981) 290.